

Calcium carbonate saturation states in the waters of the Canadian Arctic Archipelago and the Labrador Sea

Kumiko Azetsu-Scott,¹ Allyn Clarke,¹ Kelly Falkner,² James Hamilton,¹ E. Peter Jones,¹ Craig Lee,³ Brian Petrie,¹ Simon Prinsenber,¹ Michel Starr,⁴ and Philip Yeats⁵

Received 16 October 2009; revised 29 June 2010; accepted 29 July 2010; published 23 November 2010.

[1] Ocean acidification is predicted to occur first in polar oceans. We investigated the saturation state of waters with respect to calcite (Ω_{cal}) and aragonite (Ω_{arg}) in six sections along an Arctic outflow pathway through the Canadian Arctic Archipelago (CAA) and into the northwestern Atlantic using dissolved inorganic carbon and total alkalinity measurements from 2003 to 2005. The study area, a key region connecting the Arctic and the North Atlantic, includes Smith Sound, Barrow Strait, Baffin Bay, Davis Strait, Hudson Strait, and the Labrador Sea. The average Ω_{arg} in the Arctic outflow was 1.18 ± 0.17 in Barrow Strait and 1.31 ± 0.14 in Smith Sound, with areas where $\Omega_{\text{arg}} < 1$. The Arctic outflow through the CAA has a high content of Pacific waters, which have a low saturation state. These waters can be traced along the western Baffin Bay to Davis Strait. South of Davis Strait, this outflow is modified by mixing with slope and offshore waters of Atlantic origin and with the outflow from Hudson Strait. Despite the mixing, low saturation state water can still be identified on the southern Labrador Shelf. The aragonite saturation horizon is found at ~ 150 m in Barrow Strait; at 200 m in Baffin Bay, Davis Strait, and Hudson Strait; and at 2300 m in the Labrador Sea. This study provides baseline data of the saturation states for the waters of the CAA and the northwest Atlantic. It also illustrates the downstream evolution of low saturation state Arctic outflow in the northwest Atlantic.

Citation: Azetsu-Scott, K., A. Clarke, K. Falkner, J. Hamilton, E. P. Jones, C. Lee, B. Petrie, S. Prinsenber, M. Starr, and P. Yeats (2010), Calcium carbonate saturation states in the waters of the Canadian Arctic Archipelago and the Labrador Sea, *J. Geophys. Res.*, 115, C11021, doi:10.1029/2009JC005917.

1. Introduction

[2] About one third of the anthropogenic carbon dioxide (CO_2) released since the start of the Industrial Revolution in the 1800s has been taken up by the oceans [Sabine *et al.*, 2004]. This excess CO_2 is altering the basic ocean chemistry, specifically the marine carbonate system [Feely *et al.*, 2008]. Carbon dioxide that dissolves in the surface water forms carbonic acid. The increased concentrations of CO_2 in the atmosphere and surface ocean have led to a decrease in ocean pH by 0.1 units over the past 200 years [Caldeira and Wickett, 2003]. Observational studies over the last two

decades in the subtropical gyre in the North Atlantic have shown a decrease in pH that can be correlated to the increased dissolved inorganic carbon concentrations in the surface water [Bates, 2007]. Caldeira and Wickett [2003, 2005] used an ocean climate model to simulate the 21st century response of the ocean carbon system to the A1B, A2, B1, and B2 emission scenarios published by the IPCC [2000]. Their results project pH decreases by 2100 of 0.3–0.5.

[3] The most direct impact of a lower pH on the biota arises from lowered carbonate ion concentration in seawater. This affects organisms that form calcium carbonate (CaCO_3) shells and skeletons. Recent efforts to understand the impacts of ocean acidification on marine organisms have revealed diverse and complex responses [e.g., Fabry, 2008; Fabry *et al.*, 2008]. Further research on the responses of individual organisms and ecosystems is needed before the effects of ocean acidification can be reliably predicted.

[4] The saturation state of seawater with respect to CaCO_3 , rather than the pH or pCO_2 , has been shown to control the impacts of ocean acidification on many marine calcifying organisms [Gattuso *et al.*, 1998; Kleypas *et al.*, 1999; Langdon and Atkinson, 2005; Schneider and Erez, 2006]. The CaCO_3 saturation state (Ω) is defined as the product of the concentrations of the carbonate ion [CO_3^{2-}] and the

¹Ocean Sciences Division, Department of Fisheries and Oceans, Bedford Institute of Oceanography, Dartmouth, Nova Scotia, Canada.

²College of Oceanic and Atmospheric Sciences, Oregon State University, Corvallis, Oregon, USA.

³Applied Physics Laboratory, University of Washington, Seattle, Washington, USA.

⁴Department of Fisheries and Oceans, Institut Maurice-Lamontagne, Mont-Joli, Quebec, Canada.

⁵Ecological Research Division, Department of Fisheries and Oceans, Bedford Institute of Oceanography, Dartmouth, Nova Scotia, Canada.

calcium ion $[Ca^{2+}]$ divided by the stoichiometric solubility product (K_{sp}^*):

$$\Omega = [Ca^{2+}] \times [CO_3^{2-}] / K_{sp}^*$$

K_{sp}^* is a function of salinity, temperature [Mucci, 1983], and pressure [Millero, 1995] with a unit $[mol^2/kg^2]$. $CaCO_3$ occurs as calcite and aragonite in marine environments. These two polymorphs have different K_{sp}^* functions, but calcite is the more stable phase in the ocean. The saturation states of waters with respect to these two minerals are expressed as Ω_{cal} and Ω_{arg} . The calcium concentration is estimated from the salinity. Since the calcium-to-salinity ratio in seawater does not vary by more than 1.5%, variations in the ratio of $[CO_3^{2-}]$ to the stoichiometric solubility product primarily govern the degree of $CaCO_3$ saturation state [Feely et al., 2004]. The saturation state of seawater for $CaCO_3$ is a measure of its potential to corrode the $CaCO_3$ shells and skeletons of marine organisms. Without protective mechanisms, undersaturated seawater ($\Omega < 1$) is corrosive to calcifying organisms [Corliss and Honjo, 1981]. Furthermore, biological impairment can occur at saturation states with Ω_{arg} as high as 3.1 for some organisms such as reef building corals [Kleypas et al., 1999; Langdon and Atkinson, 2005].

[5] The polar oceans favor lower saturation states from the lower $[Ca^{2+}]$ concentration due to lower salinity and the higher K_{sp}^* due to lower temperature. Although ocean acidification is a global phenomenon, high-latitude surface waters are predicted to experience detrimental effects earliest, likely within decades [Orr et al., 2005]. McNeil and Matear [2007] assessed the sensitivity of the saturation state and pH to climate change feedbacks using a coupled atmosphere-ocean model. They demonstrated that climate feedbacks on future oceanic acidification levels are relatively small in most regions, with ocean acidification depending largely on the atmospheric CO_2 concentrations rather than the climate-induced oceanic changes. However, the high-latitude ocean in the Northern Hemisphere ($>60^\circ N$) is the exception. According to their model, decreased sea ice extent leads to greater atmosphere-ocean exchange of CO_2 , which in turn drives an accelerated decline for both pH and saturation states. Steinacher et al. [2009], in a separate model study, demonstrated that the largest pH changes will occur in Arctic Ocean surface waters, where aragonite undersaturation is projected within a decade due to freshening by precipitation and ice melt and by increased carbon uptake as the ice cover is reduced.

[6] The observations required to critically appraise such models are emerging. On the basis of data collected in the 1990s, Jutterström and Anderson [2005] showed that the aragonite saturation horizon is at ~ 2500 m and calcite saturation horizon is at ~ 4000 m in the central Arctic Ocean including Canada, Makarov, Nansen, and Amundsen basins. They noted a low degree of saturation at shelf break depths in the Canada Basin. Aragonite undersaturation in the surface water was observed in Queen Maud Gulf and Coronation Gulf, the southern part of the Canadian Arctic Archipelago, and on the Beaufort Shelf [Chierici and Fransson, 2009], and in the Canada Basin [Yamamoto-Kawai et al., 2009]. In the Chukchi Sea and the Canada Basin, Bates et al. [2009] showed aragonite undersaturation is caused by the interaction between a seasonal phytoplankton and carbon dynamics

in the subsurface waters and by sea ice melt in the surface layers.

[7] The Canadian Arctic Archipelago (CAA) and Hudson Bay are major pathways of water flow from the Arctic Ocean to the North Atlantic. Rapidly changing conditions in the Arctic, such as altered hydrological cycles, rising sea-water temperature and reduction of ice cover, impact biogeochemical cycles [Arrigo et al., 2008]. Anticipated changes in saturation states in the Arctic surface waters [Steinacher et al., 2009] will propagate downstream through the CAA southward from the Labrador Shelf to the Middle Atlantic Bight. We report the current calcite and aragonite saturation states of seawater and the depths of saturation horizons based on dissolved inorganic carbon and total alkalinity measurements from the CAA and the Labrador Sea in 2003–2005. Transects include Smith Sound, Barrow Strait, Baffin Bay, Hudson Strait, Davis Strait, and the Labrador Sea (Figure 1). Underlying mechanisms for controlling observed saturation states are discussed.

2. Materials and Methods

[8] Data were collected during 2003–2005 in the CAA and the Labrador Sea (Table 1). Water sampling used a 24-bottle rosette attached to a CTD (SeaBird SB43 or SBE 911) for all transects except Barrow Strait, where Niskin bottles were deployed on a hydrowire. Samples were analyzed for dissolved inorganic carbon (DIC) and total alkalinity (TA) on board within 24 h of collection for the Labrador Sea transect. For the other transects, the samples were collected and stored in 500 mL glass bottles following the method prescribed by DOE [1994]. Stored samples were analyzed within 6 months of collection.

[9] The DIC was determined using gas extraction and a coulometric method with photometric detection [Johnson et al., 1985]. Total alkalinity (TA) was measured by open-cell potentiometric titration with a five-point method [Haraldsson et al., 1997]. Certified Reference Material (CRM) (supplied by Professor Andrew Dickson, Scripps Institution of Oceanography, San Diego, USA) was analyzed in duplicate every 20 samples to evaluate accuracy. Precision of analyses varied on different cruises. One standard deviation from the differences of duplicate CRM measurements for DIC and TA over the cruise is summarized in Table 2.

[10] Ω_{cal} and Ω_{arg} as well as pH_{total} (in situ temperature and pressure) were calculated from the DIC and TA measurements using the CO2SYS program [Lewis and Wallace, 1998]. The equilibrium constants (K_1 and K_2) of Mehrbach et al. [1973] as refit by Dickson and Millero [1987] (hereafter $K_{1,2}(M-DM)$) were used in this calculation. Uncertainties of Ω_{cal} and Ω_{arg} based on propagated uncertainties from replicate DIC and TA measurements are at most 0.025 and 0.013, respectively.

[11] Since we did not have nutrient analyses in some sections, phosphate and silicate concentrations were not included in the calculation to maintain consistency among the sections. Errors in Ω caused by the neglect of phosphate and silicate concentrations were estimated using the data from Davis Strait and Barrow Strait sections, where we have nutrient data. Ω_{cal} and Ω_{arg} values calculated with phosphate and silicate are higher by 0.014 ± 0.004 and 0.009 ± 0.003 for Barrow Strait and 0.012 ± 0.005 and 0.008 ± 0.003 for Davis Strait. We estimate that our calculations without

Sampling locations

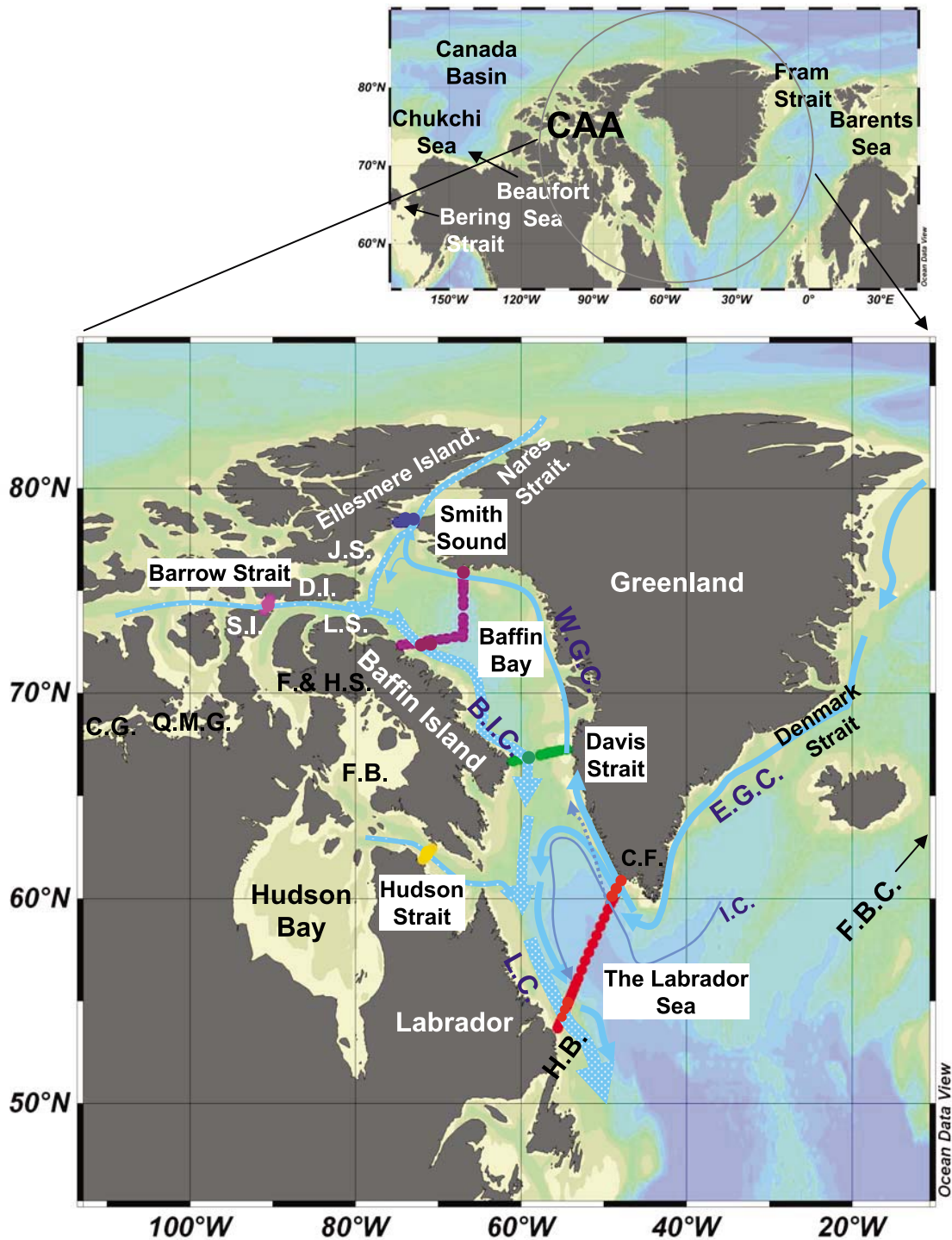


Figure 1. Sampling locations and a general surface circulation in the study area. Abbreviations: CAA, Canadian Arctic Archipelago; Q.M.G., Queen Maud Gulf; C.G., Coronation Gulf; D.I., Devon Island; L.S., Lancaster Sound; F.&H.S., Fury and Hecla Strait; J.S., Jones Sound; S.I., Somerset Island; F.B., Foxye Basin; C.F., Cape Farewell; H.B., Hamilton Bank. Blue letters indicate major currents. W.G.C., West Greenland Current; I.C., Irminger Current; E.G.C., East Greenland Current; B.I.C., Baffin Island Current; L.C., Labrador Current.

Table 1. Location, Year, Date, Number of Samples, and Names of Research Vessels for Study Data

Section	Latitude (°N) and Longitude (°W)	Year	Sampling Dates	No. of Samples	Research Vessel
Barrow Strait	(74.09, 90.44)–(74.83, 93.00)	2004	8–11 Aug	20	CCGS Pierre Radisson
Smith Sound	(78.33, 72.91)–(78.34, 74.90)	2003	2–3 Aug	27	USCGC Healy
Baffin Bay	(72.34, 66.99)–(75.84, 74.44)	2003	26–31 July	158	USCGC Healy
Davis Strait	(66.67, 54.48)–(67.26, 60.98)	2005	5–11 Sep	108	CCGS Hudson
Hudson Strait	(61.91, 71.86)–(62.44, 70.75)	2005	8–10 Sep	64	NGCC Des Groseillers
Labrador Sea	(53.68, 55.55)–(60.58, 48.22)	2003	23–29 July	453	CCGS Hudson

phosphate and silicate concentrations overestimate Ω by 0.7% for both Barrow Strait and Davis Strait.

[12] Ω variations caused by different sets of K_1 and K_2 were also evaluated using Barrow Strait and the Labrador Sea data. Ω_{arg} calculated with $K_{1,2}$ (M-DM) showed the lowest Ω_{arg} . This result agrees with the findings of *Chierici and Fransson* [2009]. Differences of Ω_{arg} with $K_{1,2}$ (M-DM) and with K_1 and K_2 by others including *Roy et al.* [1993, 1994] (hereafter $K_{1,2}$ (R)), *Goyet and Poisson* [1989], *Hansson* [1973] refit by *Dickson and Millero* [1987], *Hansson and Mehrbach* refit by *Dickson and Millero* [1987], *Mojica Prieto and Millero* [2000], and *Millero et al.* [2006] are summarized in Table 3. Discrepancies in Ω_{arg} values caused by the choice of equilibrium constants are comparable to or larger than the errors caused by the analytical precisions of DIC and TA. *Chierici and Fransson* [2009] chose $K_{1,2}$ (R), based on internal consistency, using a comparison between the calculated surface water fugacity of CO_2 ($f\text{CO}_2$) from measured TA and pH with measured $f\text{CO}_2$. Although discrepancies in Ω_{arg} values calculated using $K_{1,2}$ (M-DM) and using $K_{1,2}$ (R) decrease at lower temperature for both Barrow Strait and the Labrador Sea samples, the Barrow Strait samples showed consistently larger differences than those from the Labrador Sea (Figure 2). We could not identify the cause of this discrepancy, and further studies in different water masses are necessary to establish the best choice of K_1 and K_2 . Since we cannot test the internal consistency of our data, we chose $K_{1,2}$ (M-DM) to cover the range of water salinities and temperatures encountered in this study.

3. Water Masses and Circulation in the Arctic, CAA, and Labrador Sea

[13] At Fram Strait and the Barents Sea, Atlantic waters enter the Arctic Ocean where they form the intermediate and deepwater layers. The intermediate Atlantic layer is characterized by a temperature (0–2°C) and salinity (>34.95) maximum at a depth of several hundred meters. Winter cooling of this layer forms the Arctic bottom waters, which fill the deep basins.

[14] Pacific water enters the Arctic Ocean through Bering Strait and spreads above the Atlantic layer. In the Western Arctic, the polar mixed layer (PML) fills the surface 10–50 m, and the halocline layer extends underneath to around 230 m [*Steele et al.*, 2004]. The temperature of these layers is close to the freezing point; the vertical density gradient is maintained by salinity differences. The halocline layer is further subdivided into the upper halocline layer (UHL) or the Pacific halocline layer and the lower halocline layer (LHL) or Atlantic halocline layer [*Codispoti et al.*, 2005; *Steele et al.*,

2004]. The UHL extends to around 150 m in the Canada Basin with salinity between 31 and 33. The salinity of the LHL ranges between 34.2 and 34.6 in Beaufort Sea [*Codispoti et al.*, 2005]. The PML and the UHL are mixtures of Pacific water, freshwater from rivers, precipitation, sea ice meltwater, and brine water from sea ice formation; the LHL arises through mixing between the Atlantic layer and the UHL as these waters circulate around the Arctic Ocean.

[15] Each source of freshwater influences a different part of the Canada Basin water column. Sea ice meltwater is contained in the surface 30 m, while the salt brines created during sea ice formation have been observed at depths of up to 250 m [*Jones et al.*, 2008; *Yamamoto-Kawai et al.*, 2008]. Furthermore, river water's influence is restricted to the upper 50 m; below this depth, less saline Pacific water is the main source of the freshening of subsurface waters.

[16] The sea level difference between the Pacific and Atlantic oceans drives a flow from the Bering Strait through the Arctic into the Atlantic. Part of this flow passes through the CAA via three main channels [*Melling et al.*, 2008; *Prinsenberg et al.*, 2009]. From north to south, these are Nares Strait/Smith Sound (50 km wide at Smith Sound, a sill depth of 220 m), Jones Sound (30 km wide, a sill depth of 120 m), and Lancaster Sound/Barrow Strait (70 km wide at Barrow Strait, a sill depth of 125 m). A small portion of the water that flows through Barrow Strait bypasses Lancaster Sound and passes through the narrow Fury and Hecla Strait into Foxe Basin and thence to Hudson Bay and the Labrador Sea.

[17] Because of the shallow sill depths, most of the Arctic water which flows through the CAA originates from the PML and the UHL of the Canada Basin and Beaufort Sea. Only Nares Strait is deep enough to allow some passage of the LHL with its greater Atlantic water component. Since this study will examine the downstream modifications of the Arctic outflows, we will use the term “Arctic water” to identify waters with temperature of <0°C and salinity of <33.7. This definition follows the work of *Tang et al.* [2004] in Baffin Bay. Arctic water is mainly composed of the PML and UHL waters that have been altered by mixing with sea

Table 2. Standard Deviation for Dissolved Inorganic Carbon (DIC) and Total Alkalinity (TA) Analyses From the Differences of CRM Duplicate Measurements

Section	DIC ($\mu\text{mol/kg}$)	TA ($\mu\text{mol/kg}$)
Barrow Strait	0.44	4.49
Smith Sound/Baffin Bay	1.46	2.92
Davis Strait	1.12	4.86
Hudson Strait	0.7	3.86
Labrador Sea	0.83	1.68

Table 3. Ω_{arg} Differences Calculated From the Equilibrium Constants by *Mehrbach et al.* [1973] Refit by *Dickson and Millero* [1987] and Others for Barrow Strait and the Labrador Sea (Average \pm SD)

K_1, K_2	<i>Roy et al.</i> [1993]	<i>Goyet and Poisson</i> [1989]	<i>Hansson</i> [1973] refit by <i>Dickson and Millero</i> [1987]	<i>Hansson and Mehrbach</i> refit by <i>Dickson and Millero</i> [1987]	<i>Mojica Prieto and Millero</i> [2000]	<i>Millero et al.</i> [2006]
Barrow Strait	-0.020 ± 0.004	-0.013 ± 0.003	-0.073 ± 0.008	-0.029 ± 0.002	-0.028 ± 0.012	-0.024 ± 0.004
Labrador Sea	-0.015 ± 0.008	-0.009 ± 0.009	-0.040 ± 0.009	-0.018 ± 0.004	-0.027 ± 0.006	-0.009 ± 0.003

ice meltwater and river runoff during their passage through the CAA.

[18] The Arctic water that enters Baffin Bay through Nares Strait, Jones Sound, and Lancaster Sound is less saline and hence less dense than the interior waters of the bay. As a consequence, it forms the southward flowing Baffin Island Current (BIC) located on the continental shelf and upper slope. In the northern Labrador Sea, the BIC begins to merge with the Labrador Current. Some of its water enter Hudson Strait where it is mixed with the outflow from Hudson Bay before becoming part of the Labrador Current. This Arctic water, though modified during its southward transit by local ice formation and melting, outflow from and tidal mixing within Hudson Strait [*Straneo and Saucier*, 2008], and mixing with the saltier slope waters, still retains evidence of its Arctic (and Pacific) origin [*Jones et al.*, 2003].

[19] Arctic water also enters the North Atlantic as the East Greenland Current that flows southward along the eastern continental shelf and slope of Greenland. Because this water is leaving the Arctic far from Bering Strait, it exhibits weaker Pacific influence than CAA outflows with the variability of Pacific water content correlating significantly with the Arctic Oscillation index [*Sutherland et al.*, 2009]. Furthermore, the East Greenland Current undergoes considerable modification when it reaches Cape Farewell at the southern tip of Greenland. Part of the current mixes with warm, salty Atlantic waters to form the West Greenland Current flowing northward along the west Greenland shelf. An offshore branch, located over the upper continental slope, carries the warm and salty Irminger water northward as well (Figure 1) [*Yashayaev*, 2007]. A portion of both branches enters Baffin Bay along the eastern side of Davis Strait and contributes to the cyclonic circulation in the bay. The waters carried by these currents can be traced to northern Baffin Bay where they are found at the mouth of Nares Strait [*Tang et al.*, 2004].

[20] Arctic waters occupy the upper 100–300 m in Baffin Bay except in the southeast where the warm saline surface waters of Irminger Current origin extend northward to Disko Island (69°45'N). Most of Baffin Bay from 300 to 1200 m is filled with the West Greenland Intermediate water; parts of the basin deeper than 1200 m contain Baffin Bay deep water [*Tang et al.*, 2004].

[21] Most of the upper 2000 m of the Labrador Sea is occupied by Labrador Sea Water (LSW), which is formed by local deep convection during winter. The LSW spreads throughout the North Atlantic at the intermediate depths and is identified by a local salinity minimum. The deeper layers of the Labrador Sea contain North East Atlantic Deep Water (NEADW) from ~2300 to 3200 m and Denmark Strait

Overflow Water (DSOW) observed as a narrow layer extending 200–300 m above the bottom at depths greater than 2500 m [*Clarke and Gascard*, 1983; *Lazier et al.*, 2002; *Yashayaev*, 2007].

4. Results and Discussion

4.1. Smith Sound and Barrow Strait

[22] Low saturation states with respect to calcite and aragonite were observed in the Smith Sound and Barrow Strait sections (Figures 3 and 4). The minimum saturation state ($\Omega_{\text{arg}} < 1.2$) was at 200–300 m on the western side of Smith Sound, where *Münchow et al.* [2007] found a strong subsurface jet of Arctic outflow. The pH_{total} of the Arctic outflow was 8.06 ± 0.04 (average \pm SD) with a DIC = $2124 \pm 18 \mu\text{mol/kg}$ and a TA = $2235 \pm 12 \mu\text{mol/kg}$. These values are lower than those of surrounding waters. In contrast, the surface waters (<50 m) have a higher pH_{total} of 8.19 ± 0.08 with DIC and TA concentrations of 2008 ± 48 and $2173 \pm 20 \mu\text{mol/kg}$, respectively. It appears that biological production has consumed DIC and increased pH, thus leading to increased $[\text{CO}_3^{2-}]$ and Ω . Biological activity is also evidenced from the dissolved oxygen supersaturation in this layer. On the eastern side of the Sound, where *Münchow et al.* [2007] found the northward flowing Atlantic water, we observed a higher saturation state than the Arctic outflow.

Temperature dependency of $\Delta\Omega_{\text{arg}}$ for the Labrador Sea and the Barrow Strait

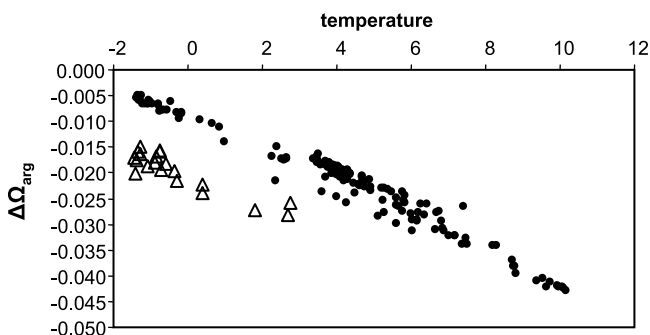


Figure 2. Temperature dependency of Ω_{arg} differences using K_1 and K_2 by *Mehrbach et al.* [1973], refit by *Dickson and Millero* [1987] ($K_{1,2}(\text{M-DM})$), and *Roy et al.* [1993] ($K_{1,2}(\text{R})$). $\Delta\Omega_{\text{arg}}$ is the difference expressed in (Ω_{arg} using $K_{1,2}(\text{M-DM})$) – (Ω_{arg} using $K_{1,2}(\text{R})$). Closed circles are for the Labrador Sea, and open triangles are for Barrow Strait.

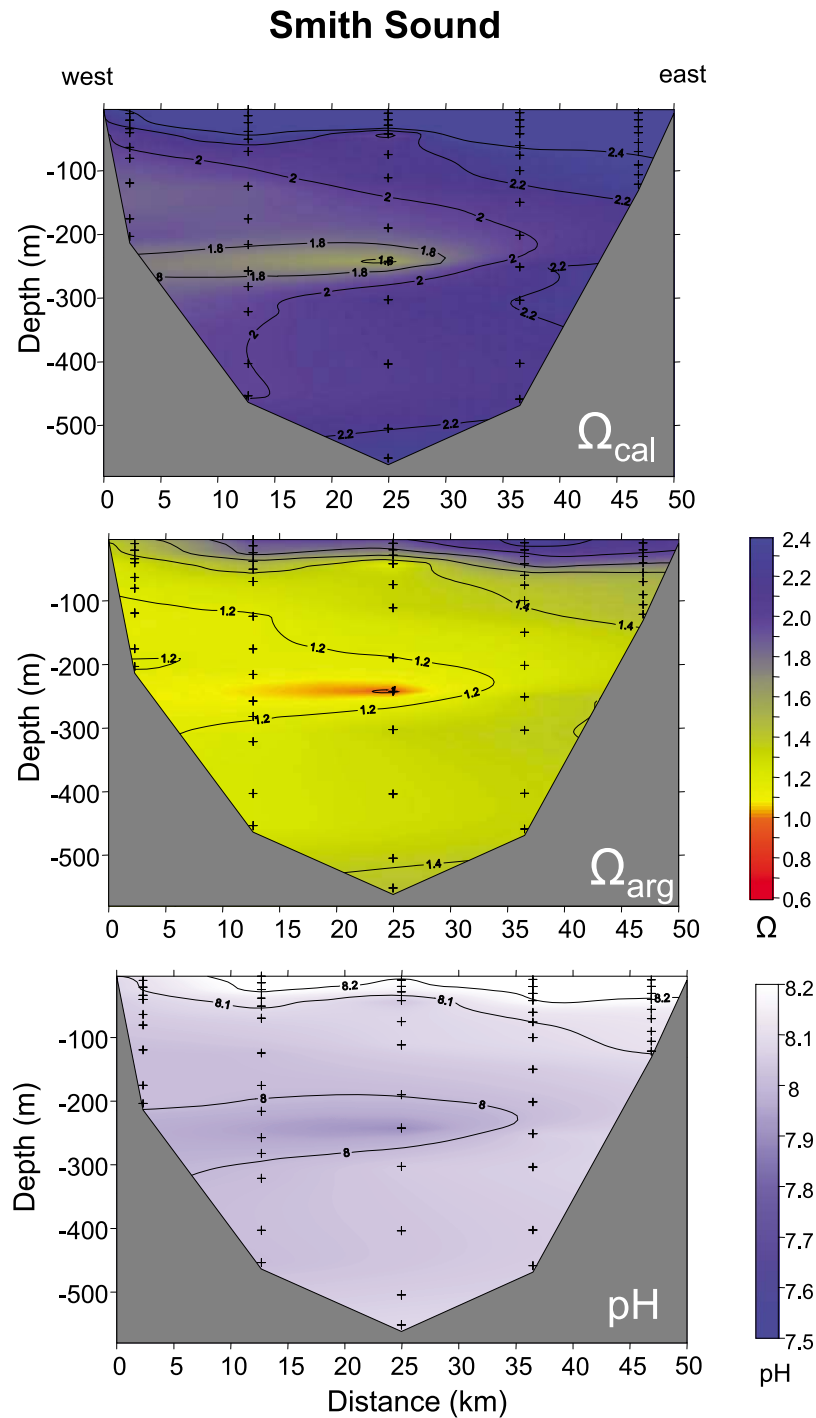


Figure 3. Saturation state for seawater with respect to calcite (Ω_{cal}) and aragonite (Ω_{arg}) and pH_{total} in Smith Sound. Plus signs indicate sampling depths. (left) Ellesmere Island and (right) Greenland.

[23] A combination of the outflow through Nares Strait and an extension of the West Greenland Current flow southward along the Ellesmere Island shelf and enters the northern side of Barrow Strait. The Arctic outflow is concentrated on the southern side of Barrow Strait [Prinsenberg *et al.*, 2009]. This is consistent with the values of $\Omega_{\text{arg}} < 1$ at 150 m at the southernmost station and at the bottom at the

adjacent station (Figure 4). Although there are only two samples with $\Omega_{\text{arg}} < 1$ and the strait was sparsely sampled, the same feature was seen in 2005 (data not shown). DIC and TA concentrations in the Arctic outflow are 2137 ± 41 and $2232 \pm 26 \mu\text{mol/kg}$ with $\text{pH}_{\text{total}} = 8.02 \pm 0.07$. In surface waters, nitrate concentrations were below the detection limit, indicative of high biological production. The DIC and

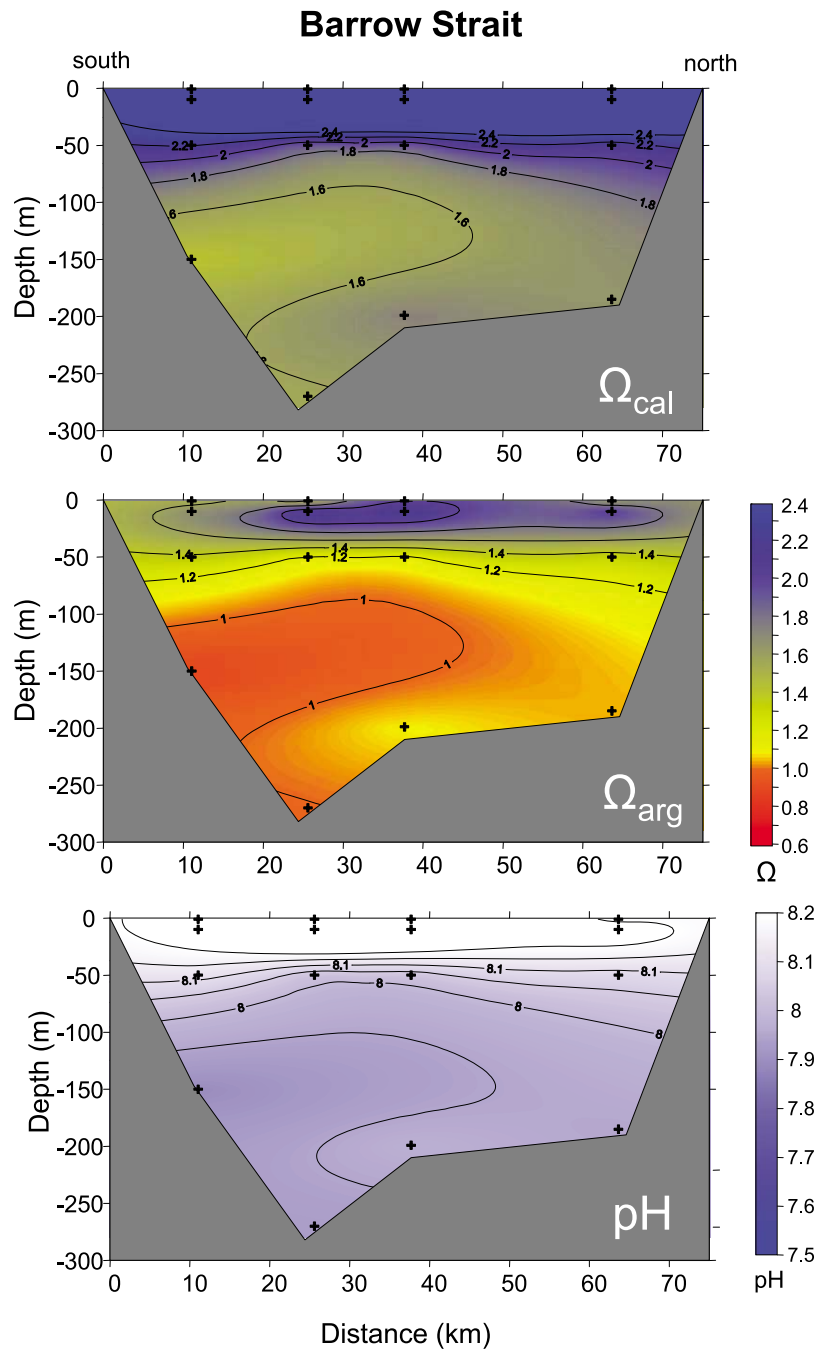


Figure 4. Saturation state for seawater with respect to calcite (Ω_{cal}) and aragonite (Ω_{arg}) and pH_{total} in Barrow Strait. (left) Somerset Island and (right) Devon Island.

TA decreased to 1925 ± 46 and $2107 \pm 67 \mu\text{mol}\cdot\text{kg}^{-1}$, respectively, while pH_{total} increased to 8.28 ± 0.07 in this surface layer. The overall distribution reflects the similar circulation pattern within both straits, namely Arctic water with low saturation states ($\Omega_{\text{arg}} < 1.2$) flows southward in Smith Sound and eastward in Barrow Strait with the shore on the right, while water with a North Atlantic component and a higher saturation state flows in the opposite direction, again with the coast on its right.

[24] Saturation states were lower in Barrow Strait than in Smith Sound. For Arctic water, Ω_{arg} in Barrow Strait was

1.18 ± 0.17 , whereas in Smith Sound, it was 1.31 ± 0.14 . Samples with nitrate concentration less than our detection limit (Barrow Strait) or $\text{AOU} < 0$ (Smith Sound) were removed from these calculations in order to eliminate samples whose Ω_{arg} have been impacted by CO_2 uptake by biological activity. A higher DIC to TA ratio in Barrow Strait causes lower pH and $[\text{CO}_3^{2-}]$ and resulted in lower Ω_{arg} . DIC and TA in Arctic outflow will be discussed in detail in section 4.5.

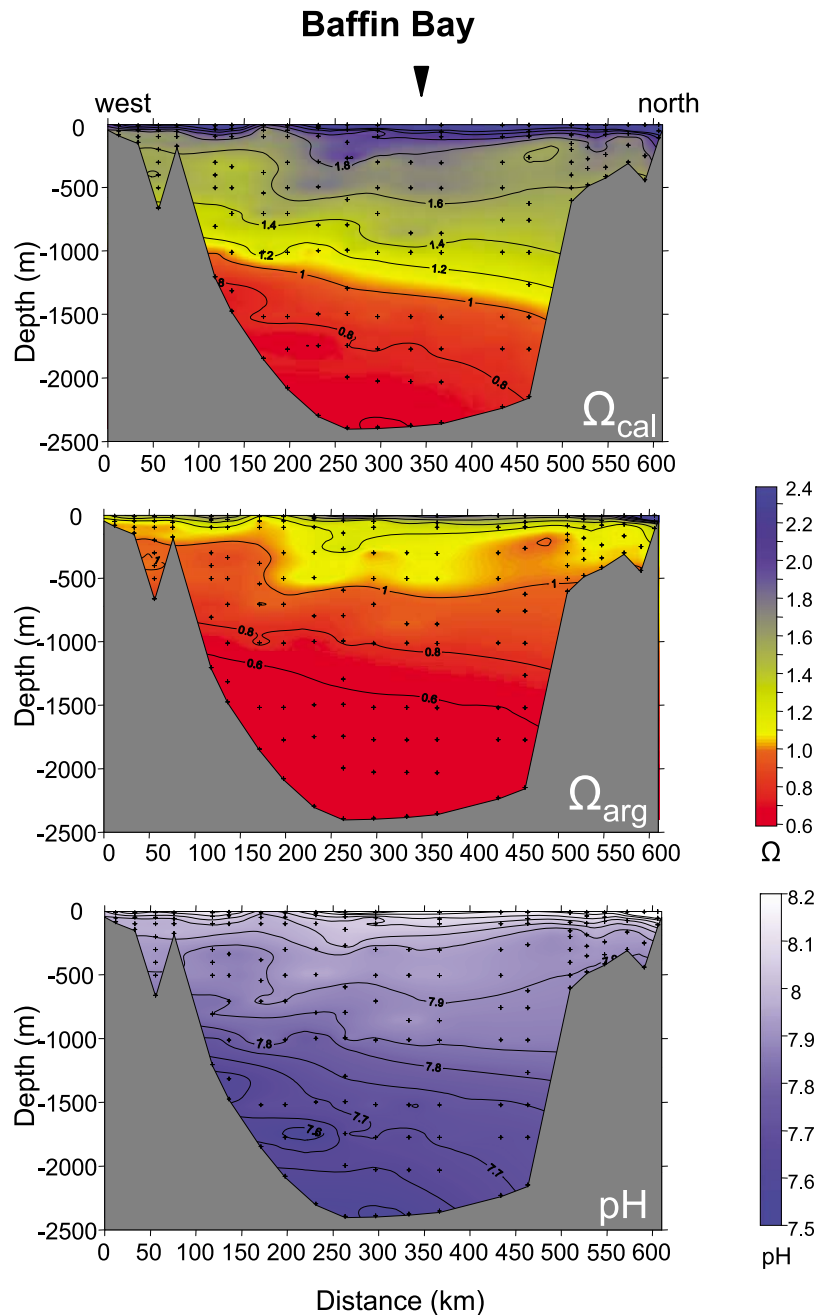


Figure 5. Saturation state for seawater with respect to calcite (Ω_{cal}) and aragonite (Ω_{arg}) and pH_{total} in Baffin Bay. (left) Baffin Island and (right) Greenland. The section continues eastward to 260 km from Baffin Island (the deepest part of Baffin Bay, indicated with solid inverted triangle) then turns northward to Greenland from 290 to 600 km.

4.2. Baffin Bay

[25] In Baffin Bay, the calcite saturation horizon ($\Omega_{\text{cal}} = 1$) was found at depths of 1000–1500 m, which corresponds to $\text{pH}_{\text{total}} = 7.75$. The aragonite saturation horizon ($\Omega_{\text{arg}} = 1$) was at depths of 200–500 m, which corresponds to $\text{pH}_{\text{total}} = 7.91$ (Figure 5). The saturation horizon deepens toward both the east and the north. On the Baffin Island Shelf, Ω_{arg} was less than 1.2 for depths >50 m. Ω_{arg} values were higher on the West Greenland Shelf than those on the Baffin Island Shelf at corresponding depths. The only undersaturated

sample ($\Omega_{\text{arg}} < 1.0$) on the West Greenland Shelf side was obtained near the bottom at 440 m. The gradient of saturation state reflects the cyclonic circulation in the bay with the addition of Arctic outflow with low saturation states at Smith, Jones, and Lancaster Sounds.

[26] While much of the Arctic water flowing through the CAA are contained on the shelves, its signature is also seen over the upper continental slope 170 km offshore of Baffin Island to depths of 500 m. This water with salinities from 32 to 33.7 and temperatures of $<0^{\circ}\text{C}$ has the same temperatures

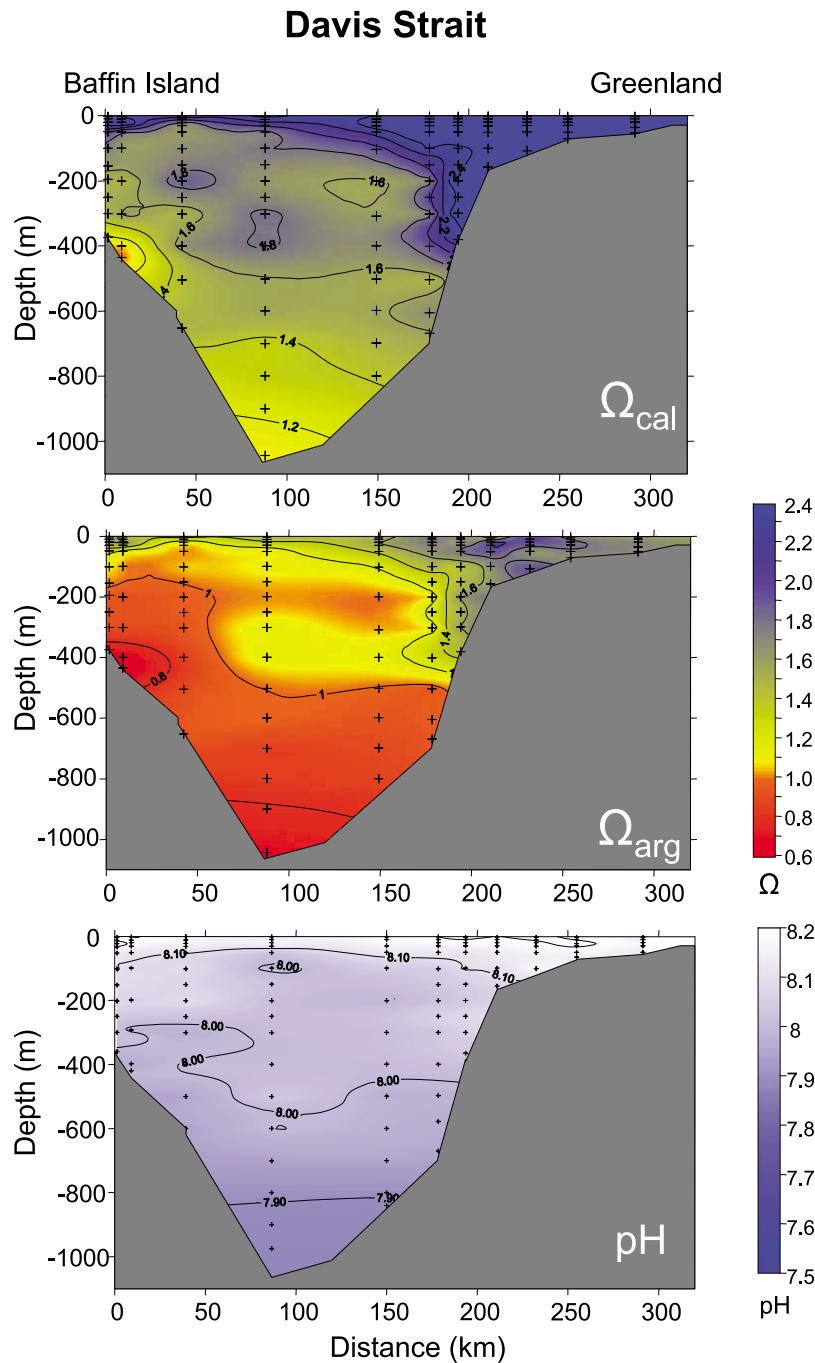


Figure 6. Saturation state for seawater with respect to calcite (Ω_{cal}) and aragonite (Ω_{arg}) and pH_{total} in Davis Strait. (left) Baffin Island and (right) Greenland. A wide continental shelf, West Greenland Shelf, is at the eastern side, while almost no continental shelf exists at Baffin Island side.

and salinities as the water identified as Arctic outflow in Barrow Strait. The Ω_{cal} and Ω_{arg} of this Arctic outflow are 1.76 ± 0.20 and $\Omega_{\text{arg}} = 1.10 \pm 0.13$. Its DIC and TA characteristics are, however, slightly different from those in Barrow Strait. DIC concentrations ($2152 \pm 12 \mu\text{mol/kg}$) are higher than those in Barrow Strait, while TA concentrations are similar ($2237 \pm 16 \mu\text{mol/kg}$). The DIC increase is due to respiration of organic matter in subsurface depths as indicated by high $f\text{CO}_2$ ($425 \pm 44 \text{ atm}$). As a result its pH_{total} at 7.99 ± 0.05 is slightly lower in the Arctic outflow in

Baffin Bay compared to those in Barrow Strait and Smith Sound.

[27] The low saturation states in the deep Baffin Bay are caused by the limited exchange of deep water in this enclosed basin. In the north, the narrow, shallow channels in the CAA limit Arctic outflows to depths less than 300 m. In the southern Baffin Bay, a 640 m deep sill at Davis Strait limits the exchange of water with the Labrador Sea. As a result, this deeper water has a long ventilation age [Top *et al.*, 1980] that has led to high DIC concentrations through respiration

Hudson Strait

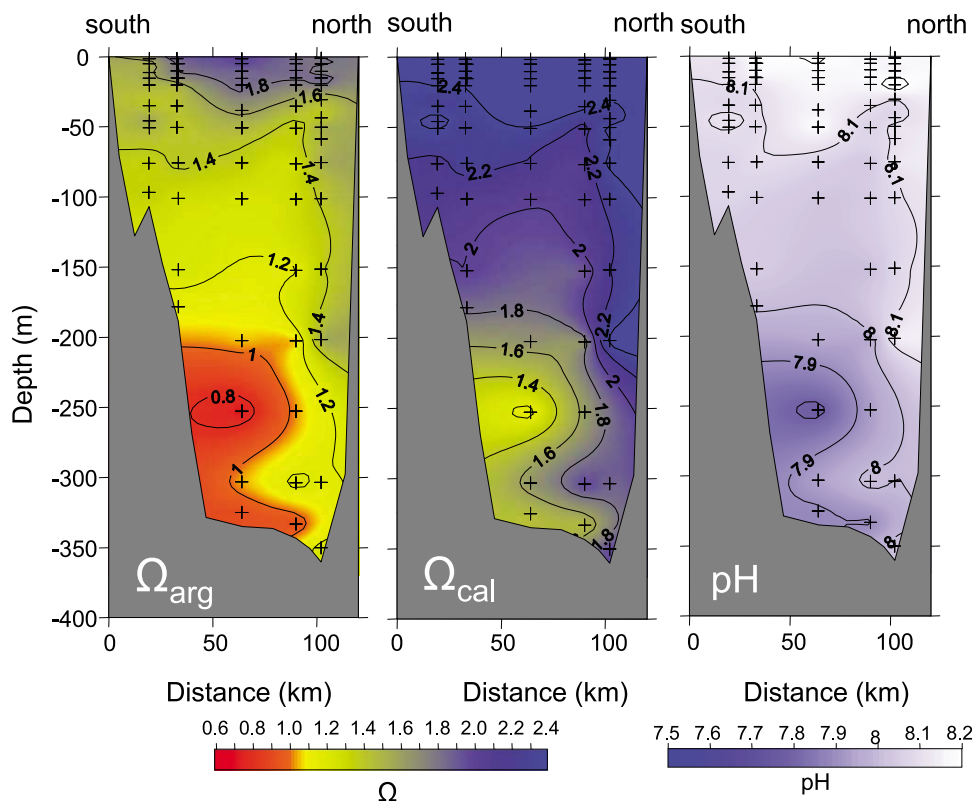


Figure 7. Saturation state for seawater with respect to calcite (Ω_{cal}) and aragonite (Ω_{arg}) and pH_{total} in Hudson Strait. (left) Labrador and (right) Baffin Island.

of organic matter. The low oxygen saturation level of $\sim 37\%$ observed in these waters is further evidence of this ongoing process. The average DIC and TA concentrations from 1000 m to the bottom in Baffin Bay are 2256 and $2292 \mu\text{mol/kg}$, while those of corresponding depths in the Labrador Sea south of the sill are 2156 and $2295 \mu\text{mol/kg}$, respectively. The accumulation of metabolic CO_2 in the deep Baffin Bay has decreased pH_{total} (7.71 ± 0.09) and $[\text{CO}_3^{2-}]$ and thus resulted in a low saturation state.

4.3. Davis Strait and Hudson Strait

[28] The Davis Strait section is located north of the sill separating Baffin Bay from the Labrador Sea. Therefore, it is not surprising that it shows a similar pattern in saturation states as seen in Baffin Bay. While the westernmost station on this section (Figure 6) is at a depth of 400 m, it is also only a few kilometers from the shore. With virtually no shelf, the Baffin Island Current (BIC) is found over the upper continental slope. The aragonite saturation horizon shallows to <200 m on the Baffin Island side and deepens to 500 m in the center and eastern end of the strait. The water at this saturation horizon has a $\text{pH}_{\text{total}} = 7.92$, similar to that observed in Baffin Bay. Values of $\Omega_{\text{cal}} \leq 1$ were observed in a limited area on the western side of Davis Strait at depths of about 400 m. As in Baffin Bay, low saturation states were associated with the Arctic outflow in the upper 300 m on the western side, extending to ~ 50 km offshore. The DIC and TA concentrations and pH_{total} of the Arctic outflow were

2152 ± 12 , 2237 ± 18 , and $7.98 \pm 0.04 \mu\text{mol/kg}$, respectively, very similar to those in Baffin Bay.

[29] Higher saturation states with $\Omega_{\text{cal}} > 2.4$ and $\Omega_{\text{arg}} > 1.6$ were observed over the wide West Greenland Shelf with $\text{pH}_{\text{total}} > 8.03$. The DIC and TA concentrations were 2076 ± 43 and $2238 \pm 38 \mu\text{mol/kg}$. The sharp gradient in saturation states over the upper continental slope separates the northward flowing shelf-slope waters entering Baffin Bay from the southward flowing waters from the bay.

[30] The hydrography and currents in the Hudson Strait have been studied by *Straneo and Saucier* [2008]. Our samples were collected on their 2005 section across the strait. According to their analysis, some of the BIC waters enter the mouth of the strait and flow toward Hudson Bay along the northern side. The mouth of the strait is an area of intense tidal mixing so that these westward flowing waters become well mixed and weakly stratified. River runoff of about $900 \text{ km}^3/\text{yr}$ augmented by sea ice meltwater leads to a stratified Hudson Bay outflow with surface salinities of <31 . This outflow is concentrated on the southern side of the strait in the upper 100 m [*Straneo and Saucier*, 2008]. The flows below 250 m are much weaker than those in the upper layers, but they generally follow the same pattern of westward flow in the north and eastward flow in the south.

[31] Our observations are consistent with this circulation pattern. The saturation values are relatively high and uniform on the northern side of the section ($\Omega_{\text{arg}} = 1.44 \pm 0.11$) (Figure 7). The BIC at Davis Strait has high saturation

values in the surface layer due to photosynthesis, evidenced by low nutrients and high oxygen concentrations, and low saturation values below 50 m. Nevertheless, mixing of the water column at the mouth of Hudson Strait raises the saturation state and results in the higher observed saturation values in the northern part of the section.

[32] In the southern part, the vertical distribution of Ω in the upper 150 m reflects the stratification in the Hudson Bay outflow. The Ω_{arg} of this surface outflow is 1.39 ± 0.10 and is the result of low DIC ($2088 \pm 34 \mu\text{mol/kg}$) and TA ($2209 \pm 26 \mu\text{mol/kg}$) concentrations and a low pH_{total} (8.08 ± 0.02), relative to the BIC inflow. The low salinity (32.02 ± 0.73) of this layer is further evidence that the observed decrease in Ω in the Hudson Strait outflow is caused by the freshwater dilution due to sea ice meltwater and river runoff.

[33] Low saturation states were also observed below 200 m ($\Omega_{\text{arg}} = 0.94 \pm 0.16$) in the southern part of the channel; these may be the result of the long residence time of these deep waters [Drinkwater, 1988], which has resulted in accumulation of DIC by organic matter respiration. The DIC and TA concentrations were 2169 ± 14 and $2236 \pm 11 \mu\text{mol/kg}$ with a high $f\text{CO}_2$ of $540 \mu\text{atm}$. This deep layer slowly flows into the Labrador Sea [Straneo and Saucier, 2008]. The aragonite saturation horizon in the southern part of the section is at ~ 200 m (Figure 7).

4.4. The Labrador Sea

[34] The aragonite saturation horizon (with $\text{pH}_{\text{total}} = 7.97$) lies around 2300 m with no clear east-west gradient; Ω_{cal} decreases to < 1.2 near the bottom (Figure 8). This pattern of saturation states reflects the distribution of water masses in the interior of the Labrador Sea. The aragonite saturation horizon corresponds to the boundary between LSW and North East Atlantic Deep Water (NEADW).

[35] The NEADW, defined by the σ_2 density surface between 36.965 and 37.040 and extending from 2300 to 3000 m, is formed through deep convection in the Nordic Seas. The water mass is modified greatly through mixing, as it descends to its spreading depth and eventually enters the Labrador Sea at core depths of 2500–3000 m [Yashayaev, 2007; Azetsu-Scott et al., 2003]. The DIC and TA concentrations for NEADW are 2156 ± 2 and $2300 \pm 7 \mu\text{mol/kg}$. The bottom layer contains Denmark Strait Overflow Water (DSOW) that also arises through convection in the Nordic Seas. It enters the North Atlantic through the Denmark Strait and undergoes significant mixing with waters that are fresher, colder, and denser than those mixed into NEADW. The DIC and TA concentrations for DSOW are 2158 ± 3 and $2295 \pm 5 \mu\text{mol/kg}$. NEADW is the oldest water mass in the Labrador Sea with a ventilation age of 11–13 years, while DSOW has an age of 5–8 years [Azetsu-Scott et al., 2005].

[36] The upper 2300 m consists of LSW, formed in the Labrador Sea through deep convection during winters. Each winter's convection mixes the surface layers of the Labrador Sea down to variable depths, injecting anthropogenic carbon directly into the intermediate layers. The late spring/early summer annual occupation of this section by Bedford Institute of Oceanography allows the depth of the annual convection to be determined. The annual convection produces a water mass with a characteristic temperature,

salinity and depth and is identified by adding the year of formation as a subscript to LSW.

[37] Convection during the winter of 2003 extended to about 500 m. This is reflected in the fairly uniform saturation values over the upper 500 m with DIC and TA concentrations of 2157 ± 3 and $2295 \pm 4 \mu\text{mol/kg}$. The rest of the LSW layer is made up of the products of the two extreme convection events of the past two decades, LSW_{1994} and LSW_{2000} [Yashayaev, 2007]. LSW_{2000} , defined by the density surfaces $36.85 < \sigma_2 < 36.88$, extended from 500 to about 1500 m; LSW_{1994} , defined by the density surfaces $36.92 < \sigma_2 < 36.95$, was found from 1800 to 2300 m in 2003. These waters have been isolated from the atmosphere since the time of formation. DIC and TA concentrations are 2154 ± 2 and 2292 ± 6 for LSW_{2000} and 2156 ± 2 and 2294 ± 5 for LSW_{1994} . LSW_{1994} and LSW_{2000} will gradually decrease their saturation levels as they accumulate DIC due to organic matter respiration. Nevertheless, a series of cold winters could replace these water masses with the newly ventilated LSW containing high concentrations of anthropogenic CO_2 . Consequently, the saturation horizon in the Labrador Sea will not shallow gradually, but it will be controlled by intermittent deeper convections, such as those observed in early 1990s, 2000, and 2008 [Våge et al., 2009; Yashayaev and Loder, 2009].

[38] Over the Labrador Shelf (< 200 m deep, < 200 km from shore), the depth averaged Ω_{cal} , Ω_{arg} , and pH_{total} for the Arctic outflow are 2.16 ± 0.164 , 1.36 ± 0.10 , and 8.08 ± 0.04 , respectively; for the West Greenland Shelf (< 100 km from Greenland shore, deeper than 50 m), these values are 2.79 ± 0.14 , 1.76 ± 0.09 , and 8.08 ± 0.04 . The Labrador Current, in part an extension of the BIC, is modified by the outflow from Hudson Strait, by local freshwater input, and by mixing with slope waters. As a result, $\Omega_{\text{arg}} > 1$ throughout the Labrador Current, but the carbonate saturation state is still lower in the Labrador Current than the West Greenland Current.

4.5. Arctic Water Outflow

[39] The changes in the aragonite saturation state over the upper 200 m as these waters pass through the CAA, Baffin Bay and into the Labrador Sea can be examined by plotting Ω_{arg} levels in temperature and salinity space (Figure 9a). Arctic water samples, defined as $T < 0^\circ\text{C}$ and $S < 33.7$ are contained within the red ellipses. This Arctic water is also characterized by a low saturation state, $\Omega_{\text{cal}} < 1.8$ and $\Omega_{\text{arg}} < 1.2$ when the samples showing the biological uptake of CO_2 are excluded. This Arctic water is seen in both the Barrow Strait and Smith Sound sections and can be traced along the western side of Baffin Bay and Davis Strait without much modification.

[40] The bottom topography along the western margin of Davis Strait causes Arctic water to extend farther eastward over deeper water and increases the potential for mixing with Irminger and West Greenland Current waters [Tang et al., 2004; Cuny et al., 2005]. The BIC waters are subject to enhanced tidal mixing at the southern end of Baffin Island and in Hudson Strait. This mixing has elevated the saturation state of the westward flowing waters at Hudson Strait to $\Omega_{\text{arg}} > 1.4$ (northern stations; Figures 7 and 9b). The Hudson Strait outflow increases the saturation state of the southward flowing Arctic water over the Labrador Shelf (Figure 9b).

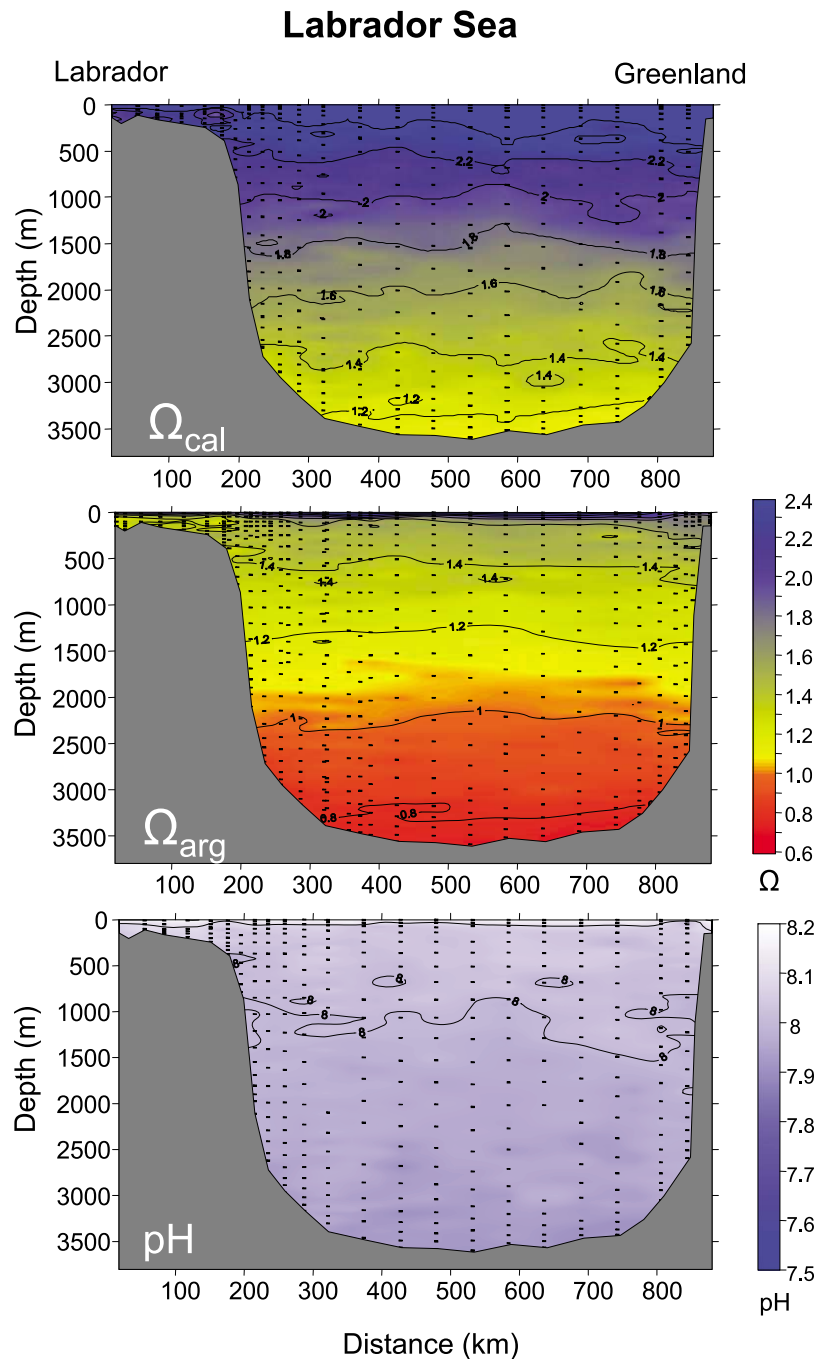


Figure 8. Saturation state for seawater with respect to calcite (Ω_{cal}) and aragonite (Ω_{arg}) and pH_{total} in the Labrador Sea. (left) Labrador and (right) Greenland.

However, this water can still be traced on the Labrador Shelf by its lower saturation state than waters in the central Labrador Sea and West Greenland Shelf (Figure 9a).

[41] The water in the West Greenland Current also has an Arctic origin. The fact that the Arctic outflows through the CAA have lower Ω than those found in the West Greenland Current is attributed primarily to a more pronounced influence of Pacific source waters in the former. Salinity and TA concentrations of the surface North Pacific are lower than those observed in the North Atlantic (Figure 10a). Table 4

shows that Ω_{arg} calculated from North Pacific data (the Bering Sea) is 1.24 ± 0.15 and pH_{total} is 7.96 ± 0.05 , whereas Ω_{arg} is 1.66 ± 0.08 and pH_{total} is 8.13 ± 0.04 in the eastern Fram Strait and $\Omega_{\text{arg}} = 1.91 \pm 0.10$ and pH_{total} is 8.11 ± 0.04 in the Barents Sea. The surface 50 m data were not included in these calculations to avoid seasonal biological influences. *Chierici and Fransson* [2009] reported Ω_{arg} ranging from 1.2 to 2.4 in shallow Bering Strait (<50 m). This relatively high Ω range represents the inflow of Pacific water to the Arctic during the short, intensive biological

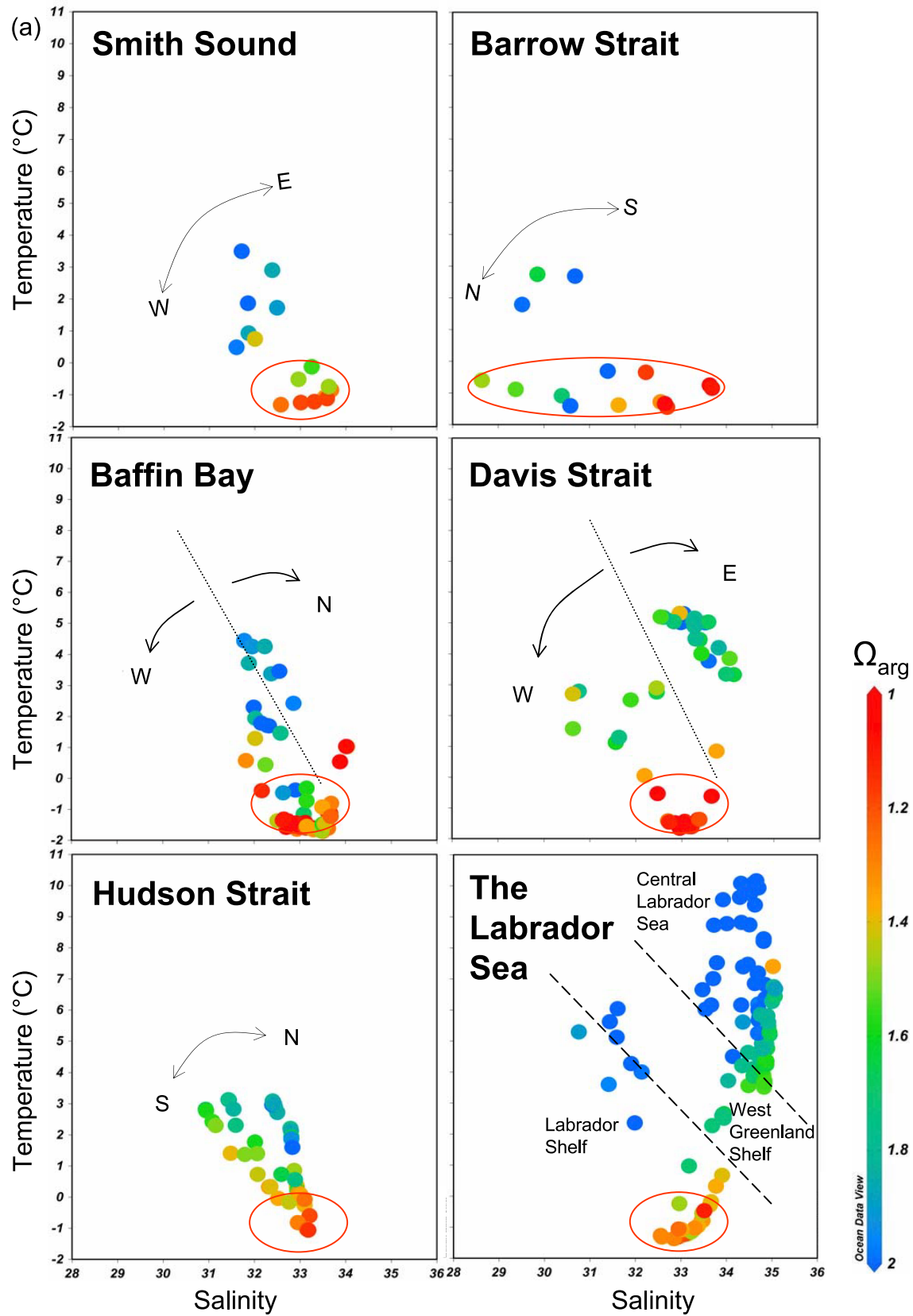


Figure 9a. Aragonite saturation state (Ω_{arg}) versus temperature and salinity for the upper 200 m samples in all sections. Red ellipses indicate Arctic water (temperature $< 0^{\circ}\text{C}$ and salinity < 33.7). E–W and S–N arrows show how the observations are distributed along the various sections. In the Labrador Sea, the samples were divided to three groups: Labrador Shelf, Central Labrador Sea, and West Greenland Shelf.

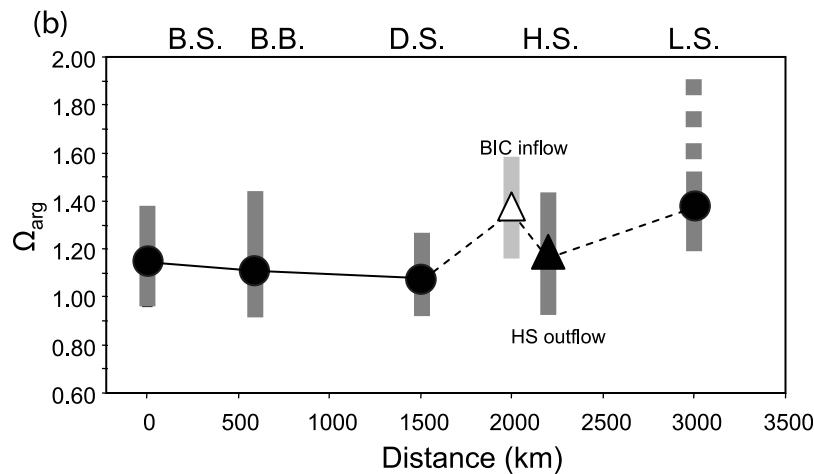


Figure 9b. Along-current evolution of Ω_{arg} in the Arctic water from Barrow Strait (B.S.), Baffin Bay (B.B.), Davis Strait (D.S.), Hudson Strait (H. S.) to the Labrador Shelf (L.S.). The Baffin Island Current (BIC) inflow to Hudson Strait (open triangle) and an outflow (solid triangle) are shown. Gray bars indicate the ranges of Ω_{arg} . A dotted bar for the Labrador Sea indicates Ω_{arg} values in the surface mixed layer where the active biological uptake of CO_2 was observed.

uptake of CO_2 period, therefore resulting in seasonal high pH and $[\text{CO}_3^{2-}]$ levels.

[42] Northern Pacific and Atlantic surface waters enter Arctic Ocean through Bering Strait and Fram Strait/Barents Sea, respectively. These waters are modified by processes such as mixing, biological activity, ice formation and melt, and river runoff. Nevertheless, both water masses tend to retain distinct distributions within the Arctic Ocean basins and as they exit through the CAA and Fram Strait. Figure 10a illustrates that waters containing high DIC concentrations in Barrow Strait and Labrador Shelf are congruent with the Pacific source while those from the West Greenland shelf and the central Labrador Sea with the Atlantic source. Figure 10a also includes a cluster of observations with low DIC and TA values in Barrow Strait and on the Labrador and West Greenland shelves. These samples have been subject to dilution by freshwater including sea ice meltwater, river runoff, glacial meltwater, and precipitation; this dilution has erased the evidence of their oceanic source, at least with regard to their DIC and TA concentrations.

[43] Freshwater inputs reduce the saturation state of the Pacific water as it flows through the Canada Basin and to the CAA. Figure 10b was constructed by using DIC and TA concentrations of $1800 \mu\text{mol/kg}$ and calcium concentration of 0.90 mmol/kg for the North American river runoff and DIC and TA concentrations of $800 \mu\text{mol/kg}$ and calcium concentration of 0.50 mmol/kg for the Siberian rivers [Telang *et al.*, 1991; Cooper *et al.*, 2008]. DIC and TA concentrations are assumed to be equal, since bicarbonate is the dominant carbonate species in the runoff [Olsson and Anderson, 1997]. The end member values for sea ice meltwater are $300 \mu\text{mol/kg}$ for DIC and TA [Anderson and Jones, 1985; Bates *et al.*, 2009; Yamamoto-Kawai *et al.*, 2009] and 0.03 mmol/kg for Ca^{2+} [Anderson and Jones, 1985]. For the seawater end member, surface (<100 m) water values from Bering Sea [Winn and Millero, 1993] (DIC = $2129 \mu\text{mol/kg}$, TA = $2227 \mu\text{mol/kg}$, Ca^{2+} = 9.69 mmol/kg) were used. Since

K_{sp}^* is valid for the salinity range of 5–44 [Mucci, 1983], freshwater fractions higher than 83% are not included. Decreases of Ω_{arg} are greatest when seawater is mixed with sea ice meltwater and least for dilution with the North American river runoff that carry higher DIC, TA, and Ca^{2+} concentrations (Figure 10b). Where the river runoff fraction is higher, the Ca^{2+} carried by rivers needs to be considered for an accurate estimate of Ω . Because of rapid changes in hydrological cycles in recent years, freshwater composition and Ω need to be investigated concurrently to better understand the future changes of ocean acidification in polar region.

[44] Pacific water entering the Canada Basin through Bering Strait is largely found in the Beaufort gyre. As a result, the Arctic outflow through the CAA contains a high Pacific water component. In an earlier study, Jones *et al.* [2003] reported that the saline end-member in the CAA is entirely of Pacific water origin. In contrast, the Pacific water component in East Greenland Current decreases rapidly from >80% in Fram Strait [Taylor *et al.*, 2003] to 15%–30% at the central part of East Greenland Shelf and to being negligible at Cape Farewell [Sutherland *et al.*, 2009]. The higher content of Pacific water in the Arctic outflow through the CAA explains its observed lower saturation state compared to the West Greenland Current, which is mainly Atlantic water.

[45] The higher Pacific water component in the Arctic outflow through Barrow Strait likely contributes to its lower saturation states compared to those observed in Smith Sound. Using the observed total inorganic nitrogen (TIN) to phosphate concentration ratio, Münchow *et al.* [2007] estimated that 25%–50% of Arctic outflow in Smith Sound in summer was of Pacific origin. Since we do not have TIN measurements in Barrow Strait, a direct comparison of Pacific water component in Arctic outflow through Barrow Strait and Smith Sound is difficult. Nevertheless, the shallower depths in Barrow Strait and a higher sill (100 m)

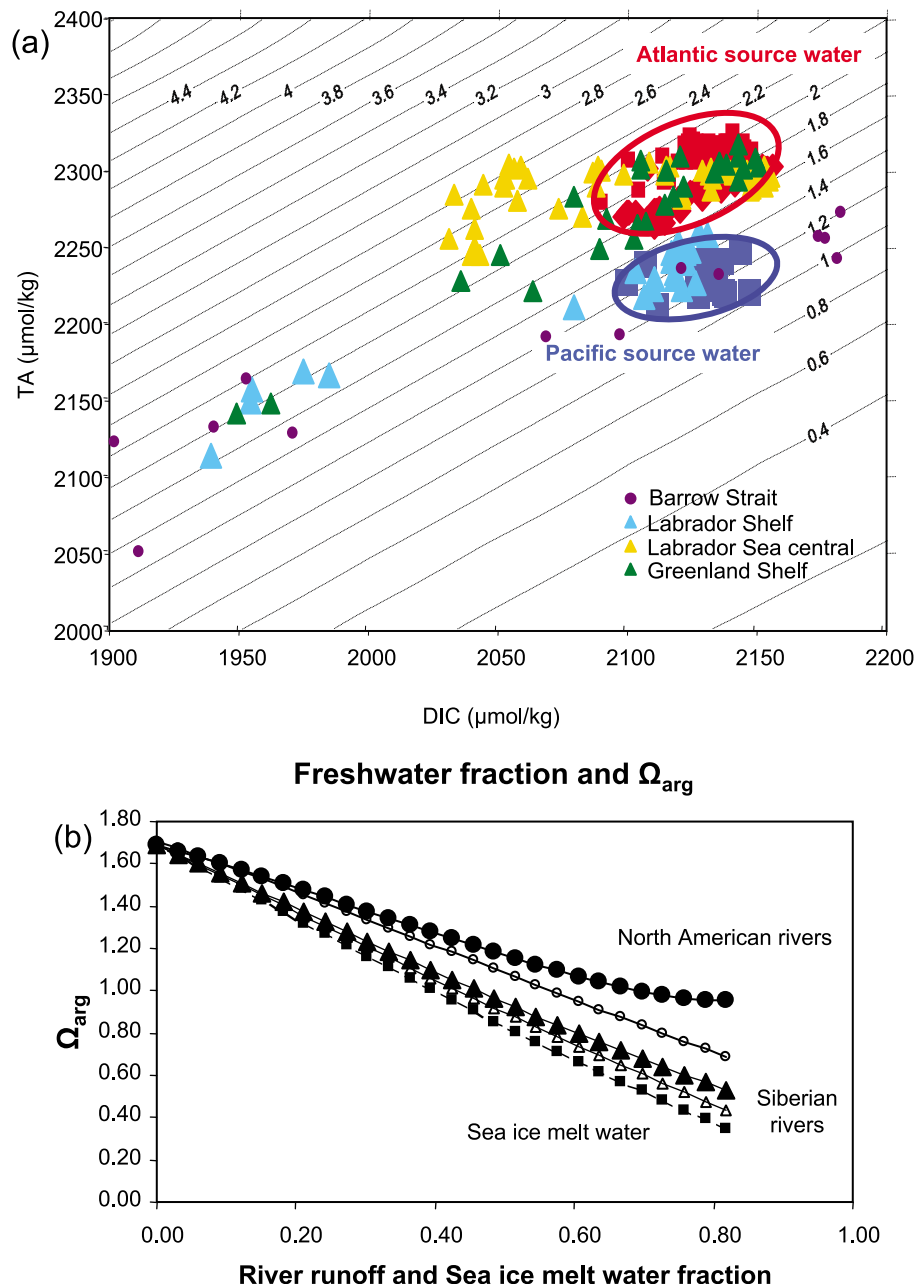


Figure 10. (a) Dissolved inorganic carbon (DIC) and total alkalinity (TA) concentrations for the different water masses. Ω_{arg} is indicated by the contours. Atlantic source water entering the Arctic via Fram Strait (red squares) [Anderson, 2007] and via the Barents Sea (red diamonds) [Bellerby and Smethie, 2007], and Pacific source waters from Bering Sea (blue squares) [Winn and Millero, 1993] are circled. Purple dots indicate samples from the Barrow Strait section. The triangles indicate the Labrador Sea samples: blue for the Labrador Shelf, yellow for the central Labrador Sea, and green for the Greenland Shelf. Ω_{arg} contours are calculated using salinity = 34, temperature = 0°C , and pressure = 1dbar. (b) Effect of dilution by different freshwater sources on Ω_{arg} . Circles indicate North American rivers, triangles indicate Siberian rivers, and squares indicate sea ice meltwater. DIC, TA, and $[\text{Ca}^{2+}]$ concentrations used for end member values are described in section 4.5. Solid marks are results that include $[\text{Ca}^{2+}]$ contribution from the rivers assuming a conservative mixing between freshwater and seawater end members. Open marks are results using $[\text{Ca}^{2+}]$ calculated from the relationship $[\text{Ca}^{2+}] = 10.28 \times (\text{salinity}/35)$ [DOE, 1994], which is used in CO2SYS program.

Table 4. Ω_{arg} and pH_{total} Calculated for the Pacific and Atlantic Source Waters Flowing Into the Arctic Ocean

Location	DIC ($\mu\text{mol/kg}$)	TA ($\mu\text{mol/kg}$)	Ω_{arg}	pH_{total}	Reference
North Pacific	2127 ± 15	2228 ± 12	1.24 ± 0.15	7.96 ± 0.05	Winn and Millero [1993]
Eastern Fram Strait	2134 ± 14	229 ± 11	1.66 ± 0.08	8.13 ± 0.04	Anderson [2007]
Barents Sea	2132 ± 11.49	2310 ± 8	1.91 ± 0.10	8.11 ± 0.04	Bellerby and Smethie [2007]

between where we collected samples in Barrow Strait and the Arctic would likely impede the flow of the denser Atlantic waters from the Arctic. It is likely that the lower saturation states observed in Barrow Strait are a consequence of a higher component of Pacific water. The DIC and TA concentrations indicate that the samples in Barrow Strait have Pacific water characteristics, and their extended range to both lower and higher DIC concentrations are evidence of strong influences of both freshwater dilution and brine rejection (Figure 10a).

5. Summary

[46] At the northern end of the study area, the average Ω_{arg} and pH_{total} in the Arctic outflow were 1.18 ± 0.17 and 8.02 ± 0.07 in Barrow Strait and 1.31 ± 0.14 and 8.06 ± 0.04 in Smith Sound, and these observations include several samples with $\Omega_{\text{arg}} < 1$. This level of saturation state is a great concern for organisms such as Arctic pelagic mollusc [Comeau *et al.*, 2009], which is an important component of marine food webs in high-latitude oceans. The advective pathway of Arctic outflow with low saturation state waters can be traced along western Baffin Bay and Davis Strait. While the outflow through Hudson Strait and local mixing in the northern Labrador Sea modifies this low Ω Arctic outflow, low saturation states can still be identified over the Labrador Shelf, at least as far south as Hamilton Bank. The low saturation state of the Arctic outflow through the CAA arises from their high content of Pacific source waters, which enter the Arctic with lower saturation states. The saturation state of this Pacific water is further decreased through the addition of sea ice meltwater and fluvial input as well as respiration of organic matter in the Arctic Ocean. The Arctic outflow appears as a low saturation state water as it enters the North Atlantic.

[47] The aragonite saturation horizons deepen from 150 m in Barrow Strait to 2300 m in the Labrador Sea. In the northern sections, strength and depth of the Arctic outflow as well as the sill depths within the different passages of the CAA control the depths of these saturation horizons. The position of the saturation horizon in the Labrador Sea is controlled by the depths of local deep convection, ventilation ages, and advective time scales of the intermediate and deepwater masses of the North Atlantic.

[48] This study provides baseline data for the saturation states of key areas in the CAA and the northwest Atlantic as well as an analysis of downstream evolution of the saturation state of the Arctic outflows through the CAA. Since the shelf regions bathed by the Arctic Ocean outflows are both biologically active and support important commercial fisheries, continued monitoring of the changes in these chemical states and investigations of biological responses to ocean acidification in this area are urgently needed.

[49] **Acknowledgments.** We are grateful to scientists of Bedford Institute of Oceanography and MERICA program of Institut Maurice-Lamontagne. This work was supported by Department of Fisheries and Oceans, International Governance Strategy program and N-CAARE high priority fund. IPY-Canada is also acknowledged for a support. K. Falkner acknowledges a support for the Healy 2003 mission of the Canadian Archipelago Throughflow Program from the Arctic Division of the Office of Polar Programs of the U.S. National Science Foundation under grant OPP-00230354. C. Lee acknowledges a support by UW ASOF program (NSF-OPP grant OPP0230381).

References

- Anderson, L. (2007), R/V Oden CARINA/77DN20020420 cruise data, CARINA Data Set, <http://cdiac.ornl.gov/ftp/oceans/CARINA/Oden/77DN0204/>, Carbon Dioxide Inf. Analysis Cent., Oak Ridge Natl. Lab., U.S. Dep. of Energy, Oak Ridge, Tenn.
- Anderson, L. G., and E. P. Jones (1985), Measurements of total alkalinity, calcium and sulfate in natural sea ice, *J. Geophys. Res.*, *90*, 9194–9196, doi:10.1029/JC090iC05p09194.
- Arrigo, K., G. van Dijken, and S. Pabi (2008), Impact of shrinking Arctic ice cover on marine primary production, *Geophys. Res. Lett.*, *35*, L19603, doi:10.1029/2008GL035028.
- Azetsu-Scott, K., R. M. Gershey, E. P. Jones, and I. Yashayaev (2003), Time series study of CFC concentrations in the Labrador Sea during deep and shallow convection regimes (1991–2000), *J. Geophys. Res.*, *108*(C11), 3354, doi:10.1029/2002JC001317.
- Azetsu-Scott, K., R. M. Gershey, and E. P. Jones (2005), Distribution and ventilation of water masses in the Labrador Sea inferred from CFCs and carbon tetrachloride, *Mar. Chem.*, *94*, 55–66.
- Bates, N. (2007), Interannual variability of the oceanic CO₂ sink in the subtropical gyre of the North Atlantic Ocean over the last 2 decades, *J. Geophys. Res.*, *112*, C09013, doi:10.1029/2006JC003759.
- Bates, N. R., J. T. Mathis, and L. W. Cooper (2009), Ocean acidification and biologically induced seasonality of carbonate mineral saturation states in the western Arctic Ocean, *J. Geophys. Res.*, *114*, C11007, doi:10.1029/2008JC004862.
- Bellerby, R., and W. Smethie (2007), Knorr 316N20020530 (Nordic "02, NS02, KN166_11) cruise data, CARINA Data Set, <http://cdiac.ornl.gov/ftp/oceans/CARINA/Knorr/316N20020530/>, Carbon Dioxide Inf. Analysis Cent., Oak Ridge Natl. Lab., U.S. Dep. of Energy, Oak Ridge, Tenn.
- Caldeira, K., and M. E. Wickett (2003), Anthropogenic carbon and ocean pH, *Nature*, *425*, 365.
- Caldeira, K., and M. E. Wickett (2005), Ocean model predictions of chemistry changes from carbon dioxide emissions to the atmosphere and ocean, *J. Geophys. Res.*, *110*, C09S04, doi:10.1029/2004JC002671.
- Chierici, M., and A. Fransson (2009), Calcium carbonate saturation in the surface water of the Arctic Ocean: Undersaturation in freshwater influenced shelves, *Biogeosciences*, *6*, 2421–2432. www.biogeosciences.net/6/2421/2009/.
- Clarke, R. A., and J.-C. Gascard (1983), The formation of Labrador Sea water: I. Large-scale processes, *J. Phys. Oceanogr.*, *13*, 1764–1778.
- Codispoti, L. A., C. Flagg, V. Kelly, and J. H. Swift (2005), Hydrographic conditions during the 2002 SBI process experiments, *Deep Sea Res., Part II*, *52*, 3199–3226.
- Comeau, S., G. Gorsky, R. Jeffree, J.-L. Teyssié, and J.-P. Gattuso (2009), Impact of ocean acidification on a key Arctic pelagic mollusk (*Limacina helicina*), *Biogeosciences*, *6*, 1877–1882. (www.biogeosciences.net/6/1877/2009/)
- Cooper, L. W., J. W. McClelland, R. M. Holmes, P. A. Raymond, J. J. Gibson, C. K. Guay, and B. J. Peterson (2008), Flow-weighted values of runoff tracers (d18O, DOC, Ba, alkalinity) from the six largest Arctic rivers, *Geophys. Res. Lett.*, *35*, L18606, doi:10.1029/2008GL035007.
- Corliss, B. H., and S. Honjo (1981), Dissolution of deep-sea benthonic foraminifera, *Micropaleontology*, *27*, 356–378.

- Cuny, J., P. B. Rhines, F. Schott, and J. Lazier (2005), Convection above the Labrador continental slope, *J. Phys. Oceanogr.*, *35*, 489–511.
- Dickson, A. G., and F. J. Millero (1987), A comparison of the equilibrium constants for the dissociation of carbonic acid in seawater media, *Deep Sea Res.*, *34*, 1733–1743. (Corrigenda, *Deep Sea Res.*, *36*, 983).
- DOE (1994), *Handbook of Methods for the Analysis of the Various Parameters of the Carbon Dioxide System in Sea Water*, ver. 2, ORNL/CDIAC-74, edited by A. G. Dickson and C. Goyet, Oak Ridge National Laboratory, Tenn.
- Drinkwater, K. F. (1988), On the mean and tidal currents in Hudson Strait, *Atmos. Ocean*, *26*, 252–266.
- Fabry, V. J. (2008), Marine Calcifiers in a High-CO₂ Ocean, *Science*, *320*, 1021–1022.
- Fabry, V. J., B. A. Seibel, R. A. Feely, and J. C. Orr (2008), Impacts of ocean acidification on marine fauna and ecosystem processes, *ICES J. Mar. Sci.*, *65*, 414–432.
- Feely, R. A., C. L. Sabine, K. Lee, W. Berelson, J. Kleypas, V. J. Fabry, and F. J. Millero (2004), Impact of anthropogenic CO₂ on the CaCO₃ system in the oceans, *Science*, *305*, 362–366.
- Feely, R. A., C. L. Sabine, J. M. Hernandez-Ayon, D. Ianson, and B. Hales (2008), Evidence for upwelling of corrosive “acidified” water onto the continental shelf, *Science*, *320*, 1490–1492.
- Gattuso, J.-P., M. Frankignoulle, I. Bourge, S. Romaine, and R. W. Buddemeier (1998), Effect of calcium carbonate saturation of seawater on coral calcification, *Global Planet. Change*, *18*, 37–46.
- Goyet, C., and A. Poisson (1989), New determination of carbonic acid dissociation constants in seawater as a function of temperature and salinity, *Deep Sea Res.*, *36*, 1635–1654.
- Hansson, I. (1973), A new set of acidity constants for carbonic acid and boric acid in seawater, *Deep Sea Res.*, *20*, 461–478.
- Haraldsson, C., L. G. Anderson, M. Hassellöv, S. Hulth, and K. Olsson (1997), Rapid high-precision potentiometric titration of alkalinity in ocean and sediment pore waters, *Deep Sea Res., Part I*, *44*, 2031–2044.
- IPCC (2000), *Emission Scenarios*, edited by N. Nakicenovic and R. Swart, pp. 570, Cambridge Univ. Press, UK.
- Johnson, K. M., A. E. King, and M. Mc Sieburth (1985), Coulometric CO₂ analyses for marine studies: An introduction, *Mar. Chem.*, *16*, 61–82.
- Jones, E. P., J. H. Swift, L. G. Anderson, M. Lipizer, G. Civitarese, K. K. Falkner, G. Kattner, and F. McLaughlin (2003), Tracing Pacific water in the North Atlantic Ocean, *J. Geophys. Res.*, *108*(C4), 3116, doi:10.1029/2001JC001141.
- Jones, E. P., L. G. Anderson, S. Jutterström, L. Mintrop, and J. H. Swift (2008), Pacific freshwater, river water and sea ice meltwater across Arctic Ocean basins: Results from the 2005 Beringia Expedition, *J. Geophys. Res.*, *113*, C08012, doi:10.1029/2007JC004124.
- Jutterström, S., and L. G. Anderson (2005), The saturation of calcite and aragonite in the Arctic Ocean, *Mar. Chem.*, *94*, 101–110.
- Kleypas, J. A., R. W. Buddemeier, D. Archer, J. P. Gattuso, C. Langdon, and B. N. Opdyke (1999), Geochemical consequences of increased atmospheric carbon dioxide on coral reefs, *Science*, *284*, 118–20.
- Langdon, C., and M. J. Atkinson (2005), Effect of elevated pCO₂ on photosynthesis and calcification of corals and interactions with seasonal change in temperature/irradiance and nutrient enrichment, *J. Geophys. Res.*, *110*, C09S07, doi:10.1029/2004JC002576.
- Lazier, J., R. Hendry, R. A. Clarke, I. Yashayaev, and P. Rhines (2002) Convection and stratification in the Labrador Sea, 1990–2000, *Deep Sea Res., Part I*, *49*, 1819–1835.
- Lewis, E., and D. W. R. Wallace (1998), Program developed for CO₂ systems calculations, ORNL/CDIAC-105, Carbon Dioxide Info. Analysis Cent., Oak Ridge Natl. Lab., U.S. Dep. of Energy, Oak Ridge, Tenn.
- McNeil, B. I., and R. J. Matear (2007), Climate change feedbacks on future oceanic acidification, *Tellus, Ser. B*, *59*, 191–198.
- Mehrbach, C., C. H. Culbertson, J. E. Hawley, and R. M. Pytkowicz (1973), Measurement of the apparent dissociation constants of carbonic acid in seawater at atmospheric pressure, *Limnol. Oceanogr.*, *18*, 897–907.
- Melling, M., T. A. Agnew, K. K. Falkner, D. A. Greenberg, C. M. Lee, A. Munchow, B. Petrie, S. J. Prinsenberg, R. M. Samelson, and R. A. Woodgate (2008), Fresh-water fluxes via Pacific and Arctic outflows across Canadian Polar Shelf, in *Arctic-Subarctic Ocean Fluxes, Defining the Role of the Northern Seas in Climate*, edited by R. R. Dickson, J. Meinke, and P. Rhines, pp. 193–247, Springer, Dordrecht, Netherlands.
- Millero, F. J. (1995), Thermodynamics of the carbon dioxide system in the oceans, *Geochim. Cosmochim. Acta*, *59*, 661–677.
- Millero, F. J., T. B. Graham, F. Huang, H. Bustos-Serrano, and D. Pierrot (2006), Dissociation constants of carbonic acid in seawater as a function of salinity and temperature, *Mar. Chem.*, *100*, 80–94.
- Mojica Prieto, F. J., and F. J. Millero (2002), The values of pK₁+pK₂ for the dissociation of carbonic acid in seawater, *Geochim. Cosmochim. Acta*, *66* (14), 2529–2540.
- Mucci, A. (1983), The solubility of calcite and aragonite in seawater at various salinities, temperatures and 1 atmosphere total pressure, *Am. J. Sci.*, *283*, 780–799.
- Münchow, A., K. K. Falkner, and H. Melling (2007), Spatial continuity of measured seawater and tracer fluxes through Nares Strait, a dynamically wide channel bordering the Canadian Archipelago, *J. Mar. Res.*, *65*, 759–788.
- Olsson, K., and L. G. Anderson (1997), Input and biogeochemical transformation of dissolved carbon in the Siberian shelf seas, *Cont. Shelf Res.*, *17*(7), 819–833, doi:10.1016/S0278-4343(96)00059-3.
- Orr, J. C., et al. (2005), Anthropogenic ocean acidification over the twenty-first century and its impact on calcifying organisms, *Nature*, *437*, 681–686.
- Prinsenberg, S. J., J. Hamilton, I. Peterson, and R. Pettipas (2009), Observing and interpreting the seasonal variability of the oceanographic fluxes passing through Lancaster Sound of the Canadian Arctic Archipelago, in *Influence of Climate Change on the Changing Arctic and Sub-Arctic Conditions*, edited by J. Nihoul and A. Kostianoy, pp. 119–137, Springer, Dordrecht, Netherlands.
- Roy, R. N., L. N. Roy, K. M. Vogel, C. Porter-Moore, T. Pearson, C. E. Good, F. J. Millero, and D. M. Campbell (1993), The dissociation constants of carbonic acid in seawater at salinities 5 to 45 and temperatures 0 to 46 °C, *Mar. Chem.*, *44*, 249–267.
- Roy, R. N., L. N. Roy, K. M. Vogel, C. Porter-Moore, T. Pearson, C. E. Good, F. J. Millero, and D. M. Campbell (1994), Erratum for: The dissociation constants of carbonic acid in seawater at salinities 5–45 and temperatures 0–45 °C, *Mar. Chem.*, *45*, 337.
- Sabine, C. L., et al. (2004), The oceanic sink for anthropogenic CO₂, *Science*, *305*(5682), 367–371.
- Schneider, K., and J. Erez (2006), The effect of carbonate chemistry on calcification and photosynthesis in the hermatypic coral *Acropora eurystoma*, *Limnol. Oceanogr.*, *51*, 1284–1293.
- Steele, M., J. Morison, W. Ermold, I. Rigor, M. Ortmeier, and K. Shimada (2004), Circulation of summer Pacific halocline water in the Arctic Ocean, *J. Geophys. Res.*, *109*, C02027, doi:10.1029/2003JC002009.
- Steinacher, M., F. Joos, T. L. Frölicher, G.-K. Plattner, and S. C. Doney (2009), Imminent ocean acidification in the Arctic projected with the NCAR global coupled carbon cycle-climate model, *Biogeosciences*, *6*, 515–533.
- Straneo, F., and F. Saucier (2008), The outflow from Hudson Strait and its contribution to the Labrador, *Deep Sea Res., Part I*, *55*, 926–946.
- Sutherland, D. A., R. S. Pickart, E. Peter Jones, K. Azetsu-Scott, A. Jane Eert, and J. Ólafsson (2009), Freshwater composition of the waters off southeast Greenland and their link to the Arctic Ocean, *J. Geophys. Res.*, *114*, C05020, doi:10.1029/2008JC004808.
- Tang, C., C. Ross, T. Yao, B. Petrie, B. DeTracey, and E. Dunlap (2004), The circulation, water masses and sea ice of Baffin Bay, *Prog. Oceanogr.*, *63*, 183–228.
- Taylor, J. R., K. K. Falkner, U. Schauer, and M. Meredith (2003), Quantitative considerations of dissolved barium as a tracer in the Arctic Ocean, *J. Geophys. Res.*, *108*(C12), 3374, doi:10.1029/2002JC001635.
- Telang, S. A., R. Pocklington, A. S. Naidu, E. A. Romankevich, I. I. Gitelson, and M. I. Gladyshev (1991), Carbon and mineral transport in major North American, Russian Arctic, and Siberian Rivers: The St. Lawrence, the Mackenzie, the Yukon, the Arctic Alaskan Rivers, the Arctic Basin Rivers in the Soviet Union, and the Yenisei, in *Biogeochemistry of Major World Rivers*, edited by E. T. Degens, S. Kempe, and J. E. Richey, pp. 75–104, Wiley, Chichester, UK.
- Top, Z., W. B. Clarke, W. C. Eismont, and E. P. Jones (1980), Radiogenic helium in Baffin Bay bottom water, *J. Mar. Res.*, *38*, 435–451.
- Våge, K., R. S. Pickart, V. Thiery, G. Reverdin, C. M. Lee, B. Petrie, T. A. Agnew, A. Wong, and M. H. Ribergaard (2009), Surprising return of deep convection to the subpolar North Atlantic Ocean in winter 2007–2008, *Nat. Geosci.*, *2*, 67–72.
- Winn, C., and F. Millero (1993), Hydrographic, Chemical and Carbon Data Obtained During the R/V Thomas Thompson cruise in the Pacific Ocean during WOCE Section P14N (EXPOCODE 325023_1), (05 July–02 September 1993), http://cdiac.ornl.gov/oceans/woce_p14n.html, Carbon Dioxide Inf. Analysis Cent., Oak Ridge Natl. Lab., U.S. Dep. of Energy, Oak Ridge, Tenn.
- Yamamoto-Kawai, M., F. A. McLaughlin, E. C. Carmack, S. Nishino, and K. Shimada (2008), Freshwater budget of the Canada Basin, Arctic Ocean, from salinity, δ¹⁸O, and nutrients, *J. Geophys. Res.*, *113*, C01007, doi:10.1029/2006JC003858.
- Yamamoto-Kawai, M., F. A. McLaughlin, E. C. Carmack, S. Nishino, and K. Shimada (2009), Aragonite undersaturation in the Arctic Ocean;

- effects of ocean acidification and sea ice melt, *Science*, 326, 1098, doi:10.1126/science.1174190
- Yashayaev, I. (2007), Hydrographic changes in the Labrador Sea, 1960–2005, *Prog. Oceanogr.*, 73, 242–276.
- Yashayaev, I., and J. W. Loder (2009), Enhanced production of Labrador Sea water in 2008, *Geophys. Res. Lett.*, 36, L01606, doi:10.1029/2008GL036162.
-
- K. Azetsu-Scott, A. Clarke, J. Hamilton, E. P. Jones, B. Petrie, and S. Prinsenber, Ocean Sciences Division, Department of Fisheries and Oceans, Bedford Institute of Oceanography, 1 Challenger Dr., PO Box 1006, Dartmouth, Canada, NS B2Y 4A2. (kumiko.azetsu-scott@dfo-mpo.gc.ca)
- K. Falkner, College of Oceanic and Atmospheric Sciences, Oregon State University, 104 COAS Admin Bldg., Corvallis, OR 97331, USA.
- C. Lee, Applied Physics Laboratory, University of Washington, 1013 NE 40th St., Box 355640, Seattle, WA 98105, USA.
- M. Starr, Department of Fisheries and Oceans, Institut Maurice-Lamontagne, Mont-Joli, QC, Canada.
- P. Yeats, Ecological Research Division, Department of Fisheries and Oceans, Bedford Institute of Oceanography, Dartmouth, Canada, NS B2Y 4A2.